Available online at www.sciencedirect.com
SCIENCE DIRECT®
Chemical Physics Letters 395 (2004) 351–355
CHEMICAL PHYSICS LETTERS
www.elsevier.com/locate/cplett

$Mo(W)_nO_m^{\pm}$ (n = 1–33; m = 2–75) clusters in the gas phase

D.M. David Jeba Singh, T. Pradeep *

Department of Chemistry and Sophisticated Analytical Instrument Facility, Indian Institute of Technology, Madras, Chennai 600 036, India

Received 24 July 2004; in final form 27 July 2004
Available online 21 August 2004

Abstract

H_2MoO_4 and H_2WO_4 upon direct laser desorption produce small clusters in the gas phase, extending up to 4500 and 7200 Da, respectively. The clustering patterns are quite similar for the two systems. The mass difference between successive peaks differ with increasing mass number as different kinds of structures become possible. A distinct planar to three-dimensional structural cross over is observed around the M_8 cluster. Possible structures of these clusters are presented. MoO_3 and WO_3 were also used as starting materials, which yielded the same clusters.

1. Introduction

Clusters are considered to constitute a new form of matter, as they have properties fundamentally different from discrete molecules and bulk solids [1]. Although the scientific study of clusters is fairly recent, they have been around for a long time, giving color to stained glass windows, for example. One of the most important reasons for studying clusters is that they exist in a wide range of sizes with diverse properties. There is considerable interest in the study of gas phase metal oxide clusters such as understanding of chemical reactivity and catalysis. Formation of gas phase clusters is monitored by mass spectrometric techniques, which provide valuable information on their stability. For the gas phase generation of clusters, a number of methods have been explored during the past decades, such as evaporation of metals by heating and laser or ion bombardment. However, laser vaporization technique has been widely accepted for the production of metal clusters, especially in conjunction with mass spectrometry [2–4]. Recently, the generation of high aggregation number silver clusters under matrix-assisted laser desorption ionization (MALDI) conditions using silver salts and reductive polar organic matrices has been reported [5,6]. Studies of metal oxide clusters have shown that they exhibit a rich variation in properties with composition [7].

In this Letter we discuss the formation of gas phase clusters of molybdenum oxide and tungsten oxide by direct laser desorption ionization (DLDI) and MALDI. Chemical reactivity of molybdenum oxide ions with alcohols [8–10], alkanes [11] and chalcogenides [12] has been investigated in the gas phase. Similar studies have been conducted on small molybdenum cluster ions as well [9]. Many of the gas phase investigations of metal oxides are directed towards an understanding of the catalytic chemistry of the bulk systems [13]. Larger molybdenum oxide cationic clusters decompose via $(MoO_3)_n$ loss [14]. In spite of all these investigations, there are very few studies on larger clusters. There are very few studies on negatively charged clusters. In the study of Aubriet and Muller [15], positively charged clusters, $M_nO_{3n}^+$ (up to n = 1,2,...,6) were observed. They found two kinds of cluster ions. The first ones are largely oxygen-deficient and the second ones are of $M_nO_{3n}^+$, $M_nO_{3n-2}^+$ and $M_nO_{3n-1}^+$ stoichiometry (with M = Cr, Mo, and W and n = 1,2,...,6). Negatively charged MoO_3 clusters have been reported by Maleknia et al. [16] and Wang et al. [17]. Both papers clearly indicate

* Corresponding author. Fax: +91 44 22570509/0545.
E-mail address: pradeep@iitm.ac.in (T. Pradeep).

0009-2614/$ - see front matter © 2004 Elsevier B.V. All rights reserved.
doi:10.1016/j.cplett.2004.07.105

the formation of $(MO_3)_n^-(n \leqslant 6)$ anions by electron-capture processes and by dissociative electron attachment. Formation of molybdenum trioxide polymeric gaseous species by sublimation has been reported sometime ago [18]. The construction of mesoscopic species with functional properties by the derivatization of molybdenum oxide 'Giant-Wheel' clusters was reported by Cronin et al. [19]. Positively charged small tungsten oxide clusters have been reported by Muller and colleague [15]. Some of the previously listed papers also refer to tungsten oxide clusters [11,15].

There are several computational studies on Mo–O clusters. The $MoO_x^+(x = 13)$ clusters have been investigated in a combined experimental and theoretical approach by Kretzschmar et al. [12]. Fialko et al. [20] used a simple pair-potential model to calculate energy-optimized structures of molybdenum oxide cluster ions in the gas phase. This crude model predicted MoO_2^+ and MoO_3^+ clusters to be linear and trigonal planar, respectively. Duarte and co-workers [21] conducted a density functional theory study of Mo_xO_y and $Mo_xO_y^+$ clusters (x = 1–3; y = 1–9). Clusters of different conformations and multiplicities have been optimized in this study. It has been shown that MoO_3, MoO^+, MoO_2^+ and MoO_3^+ are the building blocks of larger metal clusters. This Letter is a continuation of our ongoing investigations of monolayer protected clusters in the gas phase [22] and condensed phase [23–25].

2. Experimental

Chemicals used for our work were purchased from Aldrich and were used without further purification. The mass spectrometric studies were conducted using a Voyager DE PRO Biospectrometry Workstation (Applied Biosystems) MALDITOF MS instrument. A pulsed nitrogen laser of 337 nm was used (maximum firing rate: 20 Hz, maximum pulse energy: 300 μJ) for MALDI and TOF was operated in the delayed extraction mode. For the mass spectrometric study, H_2MoO_4 (or H_2WO_4) and MoO_3 (or WO_3) were dispersed in acetone or water and spotted on the target plate. Typical delay times employed were of the order of 75–200 ns. The mass spectra were collected in both the negative and positive ion modes and were averaged for 100 shots. Most of the measurements were done in the linear TOF mode. DLDI studies were carried out to understand clustering behavior. The role of matrices on clustering has been analyzed by a series of experiments using different matrices such as 2-(4-hydroxyphenyl) azobenzoic acid (HABA), α-cyano-4-hyhroxycinamic acid (CHCA), *trans*-3-indoleacrylic acid (IAA), 2,5-dihydroxybenzoic acid (HBA) sinapinic acid (SINA), and 5-chloro salicylic acid (CSA). The cluster compound and matrices were dispersed in tetrahydrofuran (THF). We used both the negative and positive modes for acquiring the spectra. For fragmentation as well as clustering studies we used timed ion selector, which is basically an electronic gate called 'Bradbury–Nielsen gate' by which we can select particular m/z and study its metastable decay [26]. The mass selection has an uncertainty of ±4 Da.

3. Results and discussion

We investigated H_2MoO_4 first. For negative ions, the clusters are separated by m/z 146 and 164 due to MoO_3^- and MoO_4^- species, respectively. However, for positive ions, the peak spacing is m/z 130 due to MoO_2^+. The spectra are shown in Fig. 1a,b. From the spectra it can be seen that MoO_3 and MoO_4 additions occur in the negative ions, which make clusters up to $Mo_{33}O_{74}^-$ while MoO_2^+ addition occurs in the positive ion mode making clusters up to $Mo_6O_{17}^+$. Isotope pattern was clearly discernable in all the cluster peaks and a comparison of the expected [27] and observed patterns was used to assign the peaks.

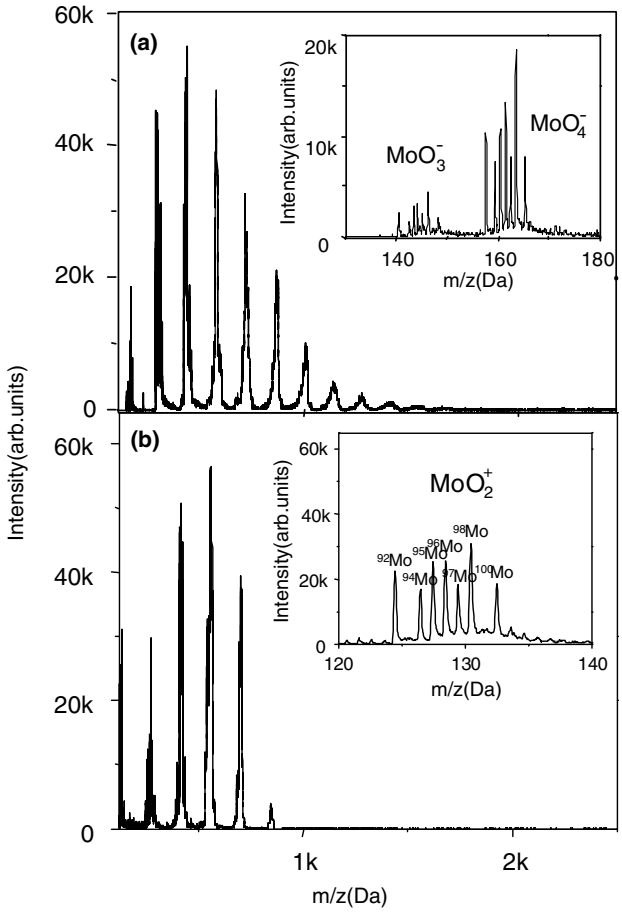

Fig. 1. The DLDI mass spectra of H_2MoO_4 in the (a) negative and (b) positive modes. Inset of (a) shows an expanded view of the MoO_3^- and MoO_4^- peaks showing the isotope distribution. The Inset of (b) shows an expanded view of the MoO_2^+ peak.

In the negative ion mode, cluster nucleation occurs by MoO_3^-. This was proved using the timed ion selector. When *m*/*z* 146 alone was allowed to pass by applying the Bradbury–Nielsen gate, the mass spectrum (Fig. 2) shows all the clusters observed in the normal mass spectrum (also shown in Fig. 2). This indicates that clusters are formed by MoO_3 species in the negative ion mode. A significant portion of the parent MoO_3^- ions got converted to higher analogues, however, with a different intensity distribution. This occurs as MoO_3^- undergoes ion-molecule association reaction with the neutrals formed in the flight region. The lesser intensity peaks such as $Mo_2O_7^-$, $Mo_3O_{10}^-$, and $Mo_4O_{13}^-$ (in Fig. 1a) suggest that MoO_4 is also involved in clustering. Ion selected mass spectrum of MoO_4^- was similar to that of MoO_3^-.

Larger clusters do fragment in the flight region of the mass spectrometer. This is evident in the spectrum of *m*/*z* 1008 ($Mo_7O_{21}^-$, the most abundant peak due to the ion was calculated [27]) with the mass gate, which shows all the lower mass number peaks. It is important to mention that while all the clusters (from $Mo_4O_{12}^-$ to $Mo_8O_{23}^-$ show fragmentation of the kind manifested by *m*/*z* 1008; only MoO_3^- shows intense clustering. This suggests high efficiency of association reactions of the kind, $MoO_3^- + MoO_3 \rightarrow Mo_2O_6^-$. It is important to note that ions such as $Mo_8O_{23}^-$ and $Mo_8O_{25}^-$ are also observed to a lesser extent indicating the possibility of addition reactions with MoO_2 as well.

We used different matrices to study the clustering efficiency. While IAA enhances the cluster intensity, it is least with CSA. All the matrices gave similar spectra.

On the basis of the spectra, we assigned the peaks to various ions and proposed likely structures. Upon assigning the molecular formulae, we found that two kinds of structural patterns occur. Lower mass number clusters seem to exist in a two-dimensional form while the higher ones exist in a three-dimensional form. The MoO_3 and MoO_4 fragments formed during laser desorption initiate clustering and result in clusters of the kind $Mo_2O_6^-$(288), $Mo_2O_7^-$(304), $Mo_3O_9^-$(432), $Mo_3O_{10}^-$(448), $Mo_3O_{11}^-$(464), $Mo_4O_{11}^-$(560), $Mo_4O_{12}^-$(576), $Mo_4O_{13}^-$(592), $Mo_5O_{14}^-$(704), $Mo_5O_{15}^-$(720), $Mo_6O_{17}^-$(848), $Mo_6O_{18}^-$(864), $Mo_7O_{20}^-$(992), $Mo_7O_{21}^-$(1008), $Mo_8O_{23}^-$(1136) and $Mo_8O_{24}^-$(1152). The numbers given in the parentheses are mass to charge ratios (*m*/z) of the clusters. Various structural possibilities exist for these clusters. For example, one possible structure each for $Mo_7O_{20}^-$, $Mo_7O_{21}^-$, $Mo_8O_{24}^-$ and $Mo_8O_{23}^-$ are given in the Fig. 3. The structures are drawn on the basis of the solid-state structures of the constituents. We assumed triangular structure for MO_3 and tetragonal structure for MO_4. The clusters are formed through oxygen in-between two metal atoms leading to two- or three-dimensional structures. Some of the small clusters suggested here such as Mo_3O_9 are similar to the cyclic structures suggested by Duarte and co-workers [21].

The structural series seem to show a change in stability around the Mo_8 clusters. This is evident in Fig. 3. The $Mo_7O_{20}^-$ and $Mo_7O_{21}^-$ ions have similar intensity pattern as in the case of their lower mass analogues, $Mo_6O_{17}^-$ and $Mo_6O_{18}^-$. In $Mo_8O_{23}^-$ and $Mo_8O_{24}^-$, the intensity pattern is reversed which continues to higher clusters. This drastic change in the intensity distribution very clearly shows that there is a change in the stability

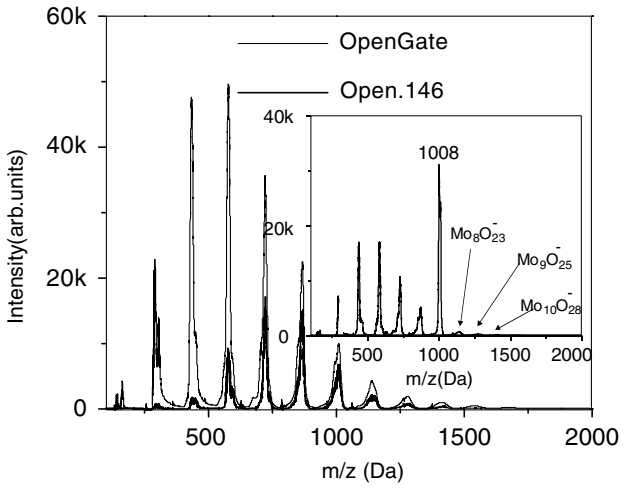

Fig. 2. DLDI mass spectrum of H_2MoO_4 in the negative mode and after applying Bradbury–Nielsen gate on *m*/*z* 146 (corresponding to $^{98}MoO_3^-$). Thin line corresponds to the spectrum without gate and thick line corresponds to the spectrum with gate. Inset shows the mass spectrum after applying gate at *m*/*z* 1008.

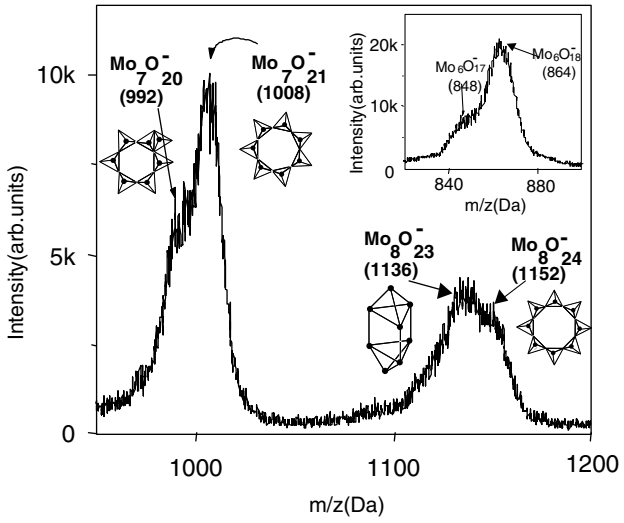

Fig. 3. The peaks which show a structural variation in the molybdenum oxide clusters. The possible structures for $Mo_7O_{20}^-$, $Mo_7O_{21}^-$ and $Mo_8O_{24}^-$ are cyclic, but for $Mo_8O_{23}^-$ it is cage-like. It is not possible to have a planar structure for $Mo_8O_{23}^-$. The structures given here are one among the probable structures. In the structures the dots indicate the Mo centers, and oxygens are not marked. In the structure of $Mo_8O_{23}^-$ Only the Mo centers are shown, for clarity. Between Mo centers binding occurs through oxygen. Inset of the figure shows that in $Mo_6O_{18}^-$ the profile is similar to $Mo_7O_{21}^-$.

of these clusters. This is interpreted as due to a change in the structure. Loss of one oxygen can change the planar structure of $Mo_8O_{24}^-$ to a close-cage structure as shown in Fig. 3. Although the structure proposed needs confirmation, a change in stability suggesting a consequent change in geometry is evident in the mass spectrum.

Using post source decay (PSD), we can study the fragmentation of particular species. The ions undergo metastable decay during the flight producing smaller ions and neutrals. Although only a single kinetic energy value is perfectly focused at a specific reflectron potential, approximately 5–10% of the entire kinetic energy range of the fragment ions can be adequately focused at this potential to produce a portion of the entire mass spectrum. It requires the reflectron potential to be systematically stepped in order to bring ions of different masses with different kinetic energies into focus. A composite mass spectrum can be produced by combining the individual portions of the mass spectrum that were produced from 10 to 20 different reflectron potential steps [28].

We studied the fragmentation of Mo_8 clusters, where we see the structural change. From the fragmentation patterns of $Mo_8O_{23}^-$ and $Mo_8O_{24}^-$ (Fig. 4) we can see the structural change from cyclic to close cage-like structure. In the PSD spectrum of $Mo_8O_{24}^-$ we see the fragment $Mo_5O_{15}^-$, which can come from a cyclic Mo_8 cluster. But in the PSD of $Mo_8O_{23}^-$ we did not see the cyclic fragment, which shows that its structure is different from that of $Mo_8O_{24}^-$. Note that all the other fragments seen in both the cases are similar, although with different intensities.

We studied the clusters in the positive mode also. Isotope patterns were used to assign the molecular formulae. Here cluster nucleation occurs principally by MoO_2^+. This was proved using the timed ion selector. When *m/z* 130 alone was allowed to pass by applying the timed ion selector, the mass spectrum (Fig. 5) shows all the clusters observed in the normal mass spectrum except $Mo_2O_4^+$ (also shown in Fig. 5 as dotted line). The clusters observed in the regular mass spectrum are $Mo_2O_4^+$(256), $Mo_2O_5^+$(272), $Mo_2O_6^+$(288), $Mo_3O_6^+$(384), $Mo_3O_7^+$(400), $Mo_3O_8^+$(416), $Mo_3O_9^+$(432), $Mo_4O_8^+$(512), $Mo_4O_9^+$(528), $Mo_4O_{10}^+$(544), $Mo_4O_{11}^+$(560), $Mo_4O_{12}^+$(576), $Mo_5O_{13}^+$(688), $Mo_5O_{14}^+$(704), $Mo_6O_{16}^+$(832) and $Mo_6O_{17}^+$(848); mass numbers are in parentheses. PSD spectrum of $Mo_6O_{17}^+$ is shown in the inset of Fig. 5. The spectrum shows extremely well-defined fragment ions suggesting that the clusters produced are isostructural. Well-defined fragment ions were seen in the PSD of all the other major peaks such as $Mo_4O_{11}^+$ and $Mo_6O_{17}^+$.

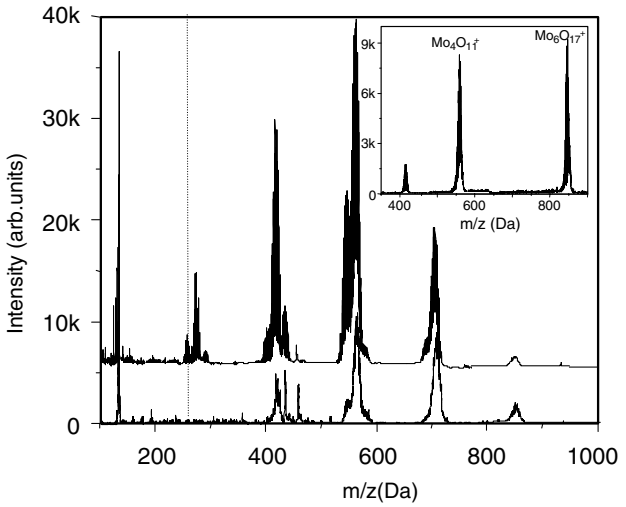

Fig. 5. DLDI mass spectrum derived from H_2MoO_4 in the positive ion mode (top trace) and after applying Bradbury–Nielson gate on *m/z* 130 (corresponding to $^{98}MoO_2^+$, bottom trace). Dotted vertical line shows the $Mo_2O_4^+$ position, which is absent in the lower trace. Inset shows the PSD mode DLDI mass spectrum after applying gate at *m/z* 852.

MoO_3 was also used as the precursor material to study cluster formation. The patterns observed were similar.

3.1. W_mO_n clusters

Similar studies were done with H_2WO_4 and WO_3. For negative ions, the clusters are separated by *m/z*

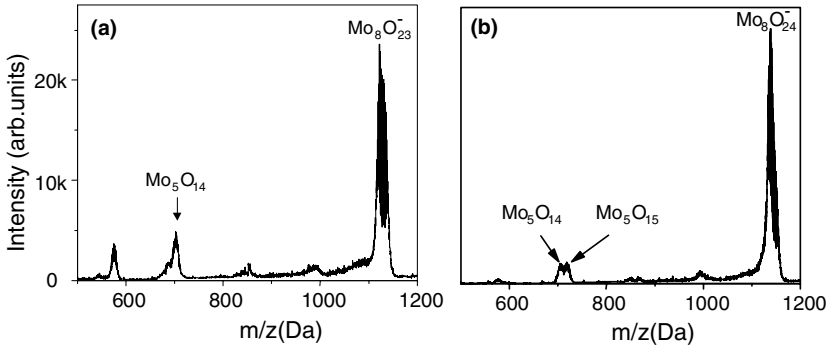

Fig. 4. PSD mode DLDI mass spectrum of (a) $Mo_8O_{23}^-$ and (b) $Mo_8O_{24}^-$ species, showing the structural change from planar to close-cage like structure.

232 and 248 due to WO_3^- and WO_4^-, respectively.However, for positive ions, the peak spacing is at *m*/*z* 216 due to WO_2^+. We used different matrices to study the clustering efficiency just as in the case of Mo clusters. While SINA enhances the cluster intensity, it is least with CSA. All the matrices gave similar spectra as in the case of DLDI.

Cluster nucleation occurs by WO_3 in the negative ion mode. This was confirmed by timed ion selector. When *m*/*z* 232 alone was allowed to pass by applying the Bradbury–Nielson gate, the mass spectrum showed all the clusters observed in the normal mass spectrum. This indicates that clusters are formed by WO_3 species, in the negative ion mode. A significant portion of the parent WO_3^- ions got converted to higher analogues, however, with a different intensity distribution. This occurs as WO_3^- undergoes ion-molecule association reaction with the neutrals formed in the flight region. Similar timed ion selector and PSD studies were conducted with positive ions also.

4. Conclusion

Laser desorption mass spectral investigation of H_2MoO_4 and MoO_3 revealed the existence of several gas phase clusters. In the negative ion mode, MoO_3 is the dominant species leading to clustering while in the positive ion mode; MoO_2 is the principal cluster forming species. Cluster formation is highly efficient with some matrices. Mass selected MoO_3^- and MoO_2^+ show clustering just as in the original mass spectra. Higher mass clusters show fragmentation as expected. From the data it appears that a structural transition, from two to three-dimensional clusters, happens around $Mo_8O_{23}^-$. The results are similar for H_2WO_4 and WO_3.

Acknowledgements

Authors thank the Department of Science and Technology for equipment support through a grant under the Nanoscience and Nanotechnology Initiative. D.M.D.J. Singh acknowledges funding from a Swarnajayanti Fellowship awarded to T.P.

References

[1] H.Y. Hang, J. Am. Chem. Soc. 125 (2003) 4388.
[2] T. Dots, M.A. Duncan, D. Powers, R.E. Smalley, J. Chem. Phys. 74 (1981) 6511.
[3] V.E. Bondebey, J.H. English, J. Chem. Phys. 76 (1982) 2165.
[4] H. Weidele, M. Vogel, A. Herlert, S. Kruckeberg, P. Lievens, R.E. Silverans, C. Walther, L. Schweikhard, Eur. Phys. J. D 9 (1999) 173.
[5] S. Keki, L.S. Szilagyi, J. Torok, G. Deak, M. Zsuga, J. Phys. Chem. B 107 (2003) 4818.
[6] H. Rashidzadeh, B. Guo, Chem. Phys. Lett. 310 (1999) 466.
[7] C.N.R. Rao, B. Raveau (Eds.), Transition Metal Oxides: Structure, Properties, and Synthesis of Ceramic Oxides, second ed., Wiley–VCH, New York, 1998.
[8] R.L. Smith, G.S. Rohrer, J. Catal. 173 (1998) 219.
[9] E.F. Fialko, A.V. Kikhtenko, B. Goncharov, Organometallics 17 (1998) 25.
[10] E.F. Fialko, A.V. Kikhtenko, V.B. Goncharov, K.I. Zamaraev, J. Phys. Chem. B 101 (1997) 5772.
[11] J.K. Gibson, J. Organomet. Chem. 51 (1998) 558.
[12] I. Kretzschmar, A. Fiedler, J.N. Harvey, D. Schroder, H. Schwarz, J. Phys. Chem. A 101 (1997) 6252.
[13] M.R. Sievers, P.B. Armentrout, J. Phys. Chem. A 102 (1998) 10754.
[14] C.J. Cassady, S.W. McElvany, Organometallics 11 (1992) 2367.
[15] F. Aubriet, J.-F. Muller, J. Phys. Chem. A 106 (2002) 6053.
[16] S. Maleknia, J. Brodbelt, K. Pope, J. Am. Soc. Mass Spectrom. 2 (1991) 212.
[17] L.F. Wang, J. Margrave, J.L. Franklin, J. Inorg. Nucl. Chem. 37 (1975) 1107.
[18] J. Berkowitz, M.G. Inghram, W.A. Chupka, J. Chem. Phys. 26 (842) (1957) 842.
[19] L. Cronin, C. Beugholt, A. Muller, J. Mol. Struct. (Theochem.) 500 (2000) 181.
[20] E.F. Fialko, A.V. Kikhtenko, V.B. Goncharov, K.I. Zamaraev, J. Phys. Chem. A 101 (1997) 607.
[21] J.A. Oliveria, W.B. De Almeida, H. Duarte, Chem. Phys. Lett. 372 (2003) 650.
[22] Jobin Cyriac, V.R. Rajeevkumar, T. Pradeep, Chem. Phys. Lett. 390 (2004) 181.
[23] T. Pradeep, S. Mitra, A. Sreekumaran Nair, R. Mukhopadhyay, J. Phys. Chem. B 108 (2004) 7012.
[24] Renjis T. Tom, V. Suryanarayanan, P. Ganapati Reddy, S. Baskaran, T. Pradeep, Langmuir 20 (2004) 1909.
[25] N. Sandhyarani, T. Pradeep, Int. Rev. Phys. Chem. 22 (2003) 221.
[26] N.E. Bradbury, R. Nielsen, Phys. Rev. A 49 (1936) 388.
[27] Using the site, available from <http://www.shef.ac.uk/chemistry/chemputer/isotopes.html>.
[28] B. Spengler, in: J.R. Chapman (Ed.), Peptide and Protein Analysis by Mass Spectrometry, Methods in Molecular Biology, vol. 61, Humana Press, Totowa, NJ, 1996.